ELSEVIER

Journal of Power Sources 94 (2001) 63–67

JOURNAL OF POWER SOURCES

www.elsevier.com/locate/jpowsour

Si–O network encapsulated graphite–silicon mixtures as negative electrodes for lithium-ion batteries

S.B. Ng[a], Jim Y. Lee[a,*], Z.L. Liu[b]

[a]*Department of Chemical and Environmental Engineering, National University of Singapore, 10 Kent Ridge Crescent, Singapore 119260, Singapore*
[b]*Institute of Materials Research and Engineering, National University of Singapore, 10 Kent Ridge Crescent, Singapore 119260, Singapore*

Received 18 August 2000; accepted 5 October 2000

Abstract

Graphite–silicon mixtures are encapsulated in a Si–O network derived from sol–gel transformation of alkoxy-silane(methyl-trimethoxy-silane). The composites are characterized by powder X-ray diffraction and scanning electron microscopy. The catalyst used in the sol–gel process significantly affects the electrochemical properties of the composites. The initial specific capacity of the composites is close to 500 mA h g^{-1}, which is between that of graphite alone (~300 mA h g^{-1}) and mechanical mixtures of graphite and silicon of identical silicon contents (~900 mA h g^{-1}). Base (NH_4OH) catalyzed composites perform substantially better than acid (HCl) catalyzed composites. The experimental results have yet to demonstrate any real advantage of the composites over graphite in terms of cycleability. Nevertheless, this approach should not be dismissed as the network material in this study may not have been optimized.

Keywords: Silicon; Graphite; Lithium-ion battery; Si–O network; Sol–gel; Negative electrode

1. Introduction

Carbon-based materials have been the material of choice for the negative electrode of lithium-ion batteries due to their excellent stability upon charging and discharging. For graphite with a low degree of turbostratic disorder, a theoretical capacity of 372 mA h g^{-1} corresponding to LiC_6 stoichiometry can be reached within 0–300 mV versus metallic Li [1].

Elements which alloy with lithium electrochemically, such as Sn, Al and Si, display higher theoretical capacities than graphite [2]. Among these elements, silicon has the highest theoretical specific capacity of ~4000 mA h g^{-1}, which corresponds to $Li_{4.4}Si$. The cycleability of Si using standard electrolytes and common separators, however, is usually poor. It is believed that the large specific volume change which accompanies charging and discharging will induce great mechanical stresses on the material and results to its pulverization [3,4].

To overcome the above problem, a number of approaches have been attempted in different studies. Wang et al. [4] reported improved cycleability and capacity from carbon–silicon mixtures prepared by extensive mechanical milling. This improvement was attributed to a reduction in the size of the Si particles which leads to a smaller absolute change in volume during cycling and thus decreases the rate of disintegration during Li intercalation and de-intercalation.

Wilson and Dahn [5] reported using chemical vapor deposition (CVD) of benzene and silicon-containing precursors (silane and derivatives) to produce nano-dispersed silicon. Due to the smaller size and better dispersion of the Si centers, the material exhibited good reversibility and capacity. The reversible capacity was reported to increase by about 30 mA h g^{-1} per (atomic) percentage point of silicon.

Bourderau et al. [3] also used CVD to produce a thin amorphous film of Si on a porous nickel substrate. In their study, carbon-based materials were not used either as active materials or as conductivity additives. Though the reported capacities for the first few cycles were high (~1000 mA h g^{-1}), the performance faded after a few cycles.

Materials for negative electrodes obtained by pyrolysis of pitch-polysilane blends have been extensive studied [6–9]. Reversible capacities for lithium insertion of ~600 mA h g^{-1}, small irreversible capacities and small hysteresis effects were reported for some of these materials. The studies showed that the materials contained nano-dispersions of Si–O–C [7,8] and Si–O–S–C [9] instead of nano-dispersed Si particles. The oxygen [8] and sulfur [9]

* Corresponding author. Tel.: +65-874-2899; fax: +65-779-1936.
E-mail address: cheleejy@nus.edu.sg (J.Y. Lee).

0378-7753/01/$ – see front matter
PII: S0378-7753(00)00603-0

contents were correlated to irreversible capacities in these studies.

In the studies mentioned above, the authors aimed to produce smaller sized silicon particles (nanosize) or a high dispersion of Si (or Si-based centers) to reduce the extent of local volume change during cycling.

Another approach has been the incorporation of another material to act as a 'cushion' for the active centers. Huang et al. [10] reported the synthesis of fine powders of tin oxide doped with traces of silicon ($Sn_xSi_{1-x}O_2$) in combination with highly dispersed amorphous silicon dioxide by flame-assisted, ultrasonic spray pyrolysis. Wang et al. [11] synthesized NiSi and FeSi alloys by mechanical milling of elemental Si and the corresponding metal powders.

In other work by Oskam et al. [12], carbon/silica gel electrodes were prepared by the sol–gel transformation of alkoxy silane precursors. The studies focused on the utilization of the gel obtained as a substitute for binder materials such as PVDF.

Previous investigations by our group [13] on mechanically mixed, gel-encapsulated-graphite and silicon powders have shown promising results. In the present investigation, graphite and silicon are encapsulated in a three-dimensional silicon oxide (–Si–O–) network which is formed by sol–gel transformation in aqueous media. We shall denote this (–Si–O–) network material as 'silica gel'. The effect of the catalyst used on the electrochemical performance of the composites is investigated. It is hoped that the cage-like structure trapping the active material will restrain the expansion and contraction of the latter during cycling, and thus will lead to improved cycle-life.

2. Experimental

2.1. Synthesis of graphite–silicon–silica network composites

Methyltrimethoxysilane of 2 ml (MTMOS, Fluka, purity >98%), 5 ml of distilled water and 0.1 ml of HCl (BDH, 37%) or 0.1 ml of ammonium hydroxide (Merck, 25%) were mixed with agitation to produce the gelation medium. Mesophase carbon of 3 g (KMFC A1500 from Kawasaki Steel Corporation) and 1 g of silicon powder (Aldrich, −325 mesh) were manually milled and mixed thoroughly before being added slowly to the gelation medium. The mixture was stirred for 2 h, left to stand at 20°C for 24 h, heated at 80°C for a further 24 h and finally left in a vacuum oven at 130°C for 2 h. The resulting composite was then manually milled to the powder form.

2.2. Estimation of the silica gel content in the composite

As the silica gel obtained is chemically inert to lithium insertion, an estimate of its content was essential for subsequent calculations. The total weight of a dry glass beaker and a magnetic stirrer was determined before the reagents were mixed. After drying in the vacuum oven, the total weight of the beaker with all its contents was measured again. The weight of silica gel could then be found by subtracting the weight of the carbon and silicon (4 g) from the total weight of the composite.

2.3. Assembly of test cells

Composite powder 80 wt.%, 5 wt.% carbon black as conductivity agent and 15 wt.% poly(vinylidene fluoride) PVDF binder were mixed in 1-methly-2-pyrrolidone (NMP) to give a slurry. This was coated on to a copper current-collector (1 cm^2) at a loading of about 6–8 mg of active material (KMFC + Si) after drying at 80°C for 24 h, compacting at 1.4×10^7 Pa, and further drying at 110°C in vacuum for 2 h.

The test electrode was assembled in a typical two-electrode test cell using lithium foil as the counter electrode, 1 M $LiPF_6$ in EC/DEC (1:1 w/w) as the electrolyte, and microporous polypropylene as the separator. The assembly was carried out in an argon-filled glove box with less than 1 ppm each of oxygen and moisture.

2.4. Electrochemical characterizations

The test cells were discharged and charged at 20°C between 0.005 and 1.5 V (versus Li^+/Li) at a constant current density of 0.2 mA cm^{-2} for the first three cycles, followed by 0.5 mA cm^{-2} for the next 30 cycles. A Maccor Series 2000 battery tester was used for this procedure.

The structures of the composites were characterized by powder X-ray diffraction (XRD) using a Siemens D6000 diffractometer, Cu Kα radiation ($\lambda = 1.542$ nm) and a scan range of 15–80°. The morphologies of the composites were examined by a JEOL JSM-T330A scanning electron microscope.

3. Results and discussion

The samples prepared, i.e. acid-catalyzed gel and base-catalyzed gel on graphite–silicon mixtures, were compared with a KMFC sample and with a mechanically mixed graphite–Si powder (25 wt.% Si, 75 wt.% KMFC). The silica gel content in the composites was about 18.7 wt.% for the acid-catalyzed sample and 18.4 wt.% for the base-catalyzed sample.

3.1. Galvanostatic tests

The charge capacities,[1] normalized by the weight of the active materials (KMFC and Si only), of various samples are

[1] Charge capacity here refers to the amount of charge per unit mass of active material due to Li^+ de-intercalation from the test electrode.

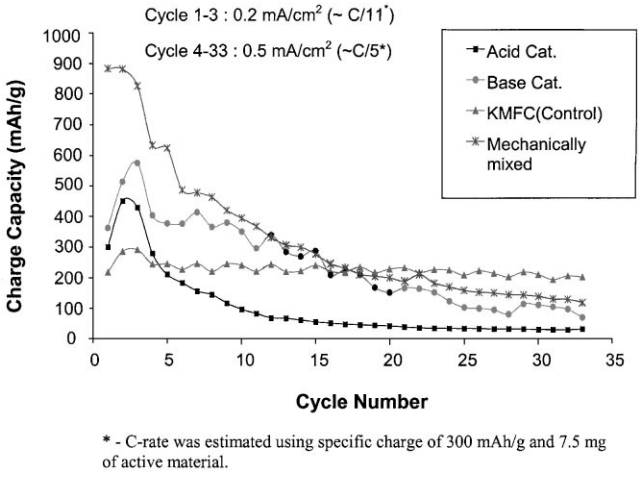

Fig. 1. Charge capacities of composites from acid-catalyzed and base-catalyzed sol–gel transformation: KMFC powder (control) and mechanically mixed KMFC–Si powder over 33 cycles.

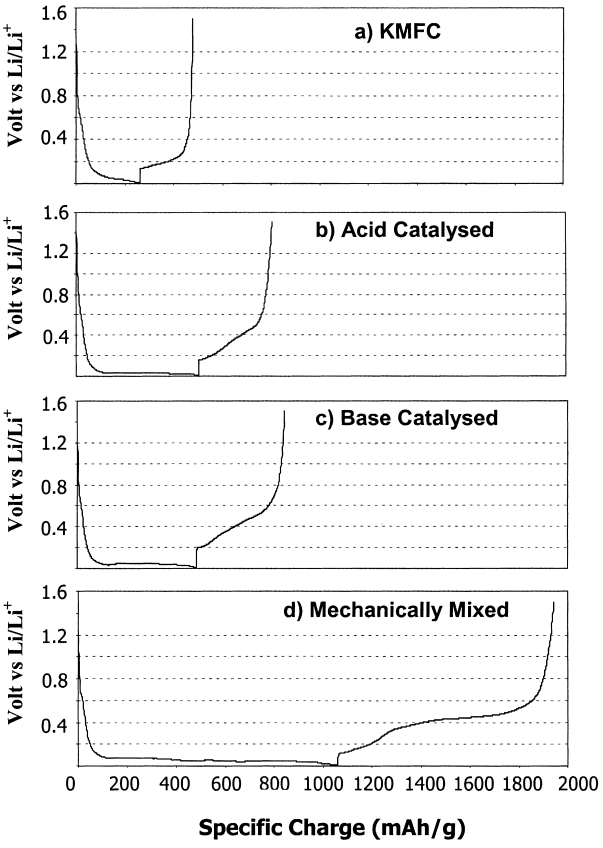

Fig. 2. First discharge and charge cycle of various active materials at current density of 0.2 mA cm^{-2}.

plotted as a function of cycle number in Fig. 1. The first three cycles show that the specific capacity of each sample (~500 mA h g^{-1}) was between that of graphite (~300 mA h g^{-1}) and a mechanically mixed graphite–Si (~900 mA h g^{-1}) electrode. For the binary Li–Si system, reversible intercalation and de-intercalation of Li^+ ions occur at stoichiometries between $Li_{1.0}Si$ and $Li_{3.5}Si$ [14]. The capacities of the samples contributed by Si correspond to approximately $Li_{1.15}Si$, whereas that of the mechanical mixture is approximately $Li_{2.82}Si$. These stoichiometries are in the stable (reversible) regime of the Li–Si system.

A sharp drop in capacity was observed for the acid-catalyzed sample upon switching to a higher current density. Overall, the base-catalyzed composite performed better than the acid-catalyzed composite upon electrochemical cycling. Gels derived from the base-catalyzed reaction are reported to have more cross-linking, whereas acid-catalyzed reactions tend to produce straight chain polymers [15]. During lithium insertion, expansion of the Si domain will lead to an increase in mechanical stress on the gel material in all directions. Thus, a cross-linked polymer network is more suited to withstand this increase in stress than a linear polymer network.

Unfortunately, the cycleabilities of the composites are far from satisfactory. After 30 cycles (Fig. 1), test cells of the composites as well as the mechanical mixture of KMFC–Si powder show reversible capacities of less than 200 mA h g^{-1}, whereas the KMFC control cell gave a capacity of ~240 mA h g^{-1}. This shows that material disintegration occurred in all the silicon-containing test cells upon cycling.

The voltage profile upon discharging and charging during the first cycle is presented in Fig. 2. From the discharge curves, it is noted that the bulk of the intercalation started at ~0.04 V versus Li/Li^+ for both composites, whereas that of KMFC or KMFC–Si started at ~0.06 V versus Li/Li^+. This is expected as the Si–O network formed on the active powders represents an extra layer of resistance and thus a more negative voltage is required to draw the positively charged Li^+ ions into the active material. The higher internal resistance (represented by the vertical portion upon transition from discharge to charge) of the composites also indicates that the Si–O network increases the overall resistance of the active materials.

Charging of the KMFC–Si mixture is marked by two characteristic plateaux at 0.1–0.2 and 0.4–0.5 V versus Li/Li^+, see Fig. 2(d). From Fig. 2(a), the plateau during charging of KMFC occurred at ~0.2 V. Thus, the plateau at 0.4–0.5 V versus Li/Li^+ represents the process of lithium de-intercalation from Si. This characteristic feature has been reported by others [4,5,13,14].

For the composites (Fig. 2(b) and (c)), the charging curves increase monotonically between ~0.2 and ~0.6 V versus Li/Li^+. A possible explanation is that, during sol–gel transformation, uniform deposition of the gel material on all particles cannot be assured. The uneven thickness of the silica network will give rise to a continuous distribution of resistance of the active particles and, for the composites, will lead to the disappearance of the two-stage plateau.

3.2. X-ray diffraction

Powder X-ray diffraction was first carried out on electrodes containing KMFC and silicon, respectively, to identify the peaks pertaining to each element. From the XRD of KMFC on a blank copper current-collector, the major peaks of KMFC were identified. The peak around 26.56° is assigned to the (0 0 2) plane of graphite [16]. Similarly, measurements of Si powder only identified the major peaks of Si (∼28.22, ∼47.1, ∼55.9, ∼68.98, and ∼76.2°) and these peaks are assigned to the various Si diffraction planes using the data [16].

The diffraction patterns of the composites given in Fig. 3 show variations in the intensities of the various peaks, but no new peaks are found. This suggests that the Si–O network is amorphous and has no effect on the crystal structure of the active powders.

3.3. Scanning electron microscopy

The various Si-containing samples at 1000× magnification are shown in Fig. 4. The particles of the mechanical mixture appear to be smaller (∼5 μm) than the particles of the chemically prepared samples (∼10 μm). Small fragments of material are more abundant in the mechanical mixture, whereas in the sol–gel derived composites, small fragments appear to be attached to agglomerated particles. Particles shown in Fig. 4(b) and (c) appear to have similar morphology.

In a study by Takamura et al. [17], the presence of small fragmented particles improved the distribution of high

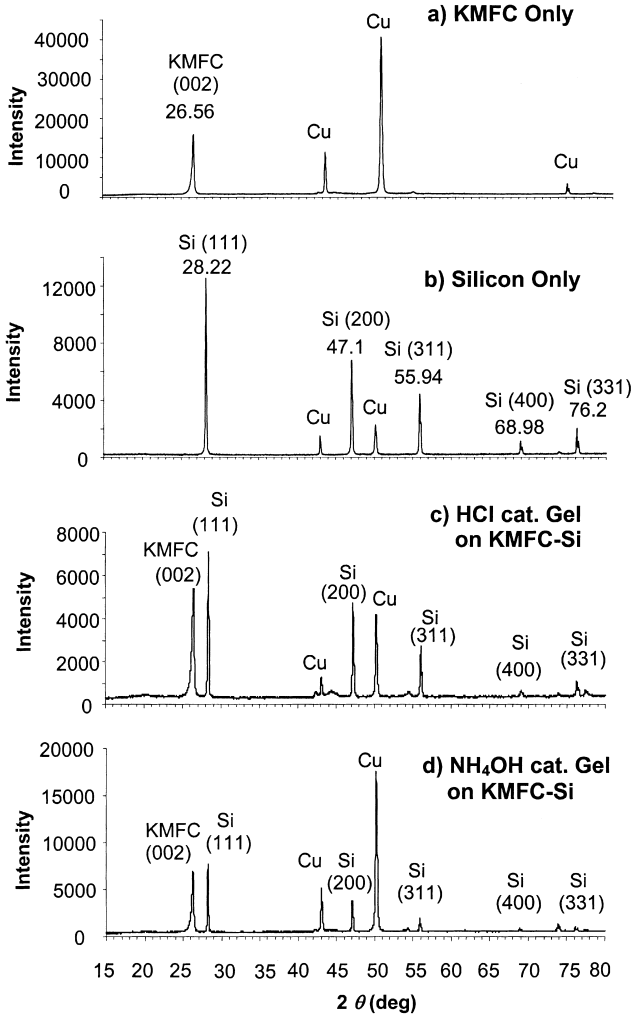

Fig. 3. Powder X-ray diffraction patterns of various active materials on a copper current-collector.

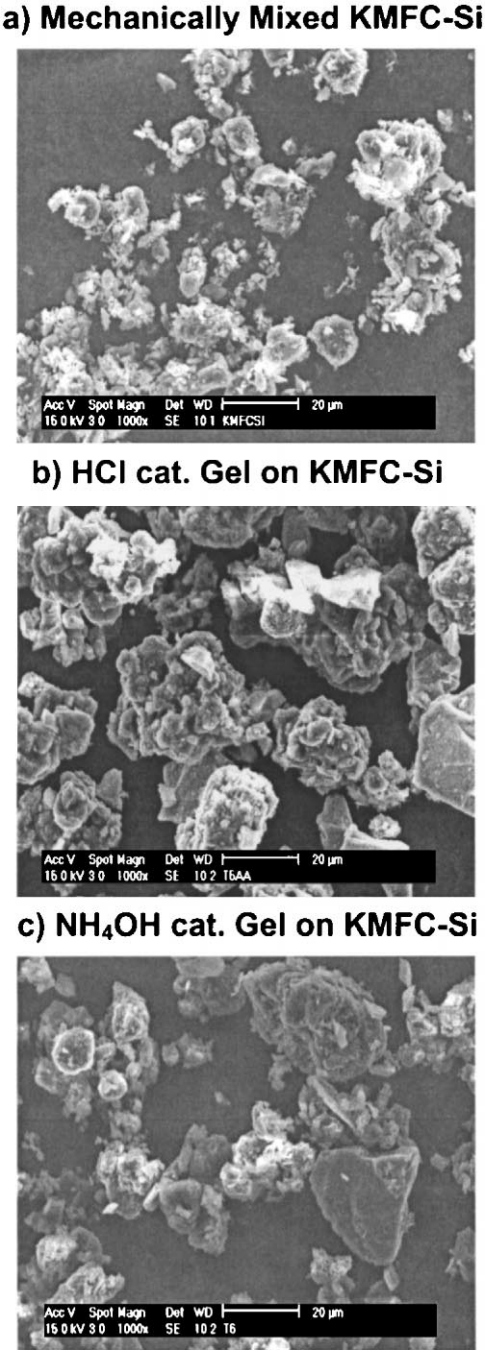

Fig. 4. Electron micrographs at 1000× magnification of: (a) mechanically mixed KMFC–Si; (b) HCl-catalyzed gel on KMFC–Si and (c) NH_4OH-catalyzed gel on KMFC–Si.

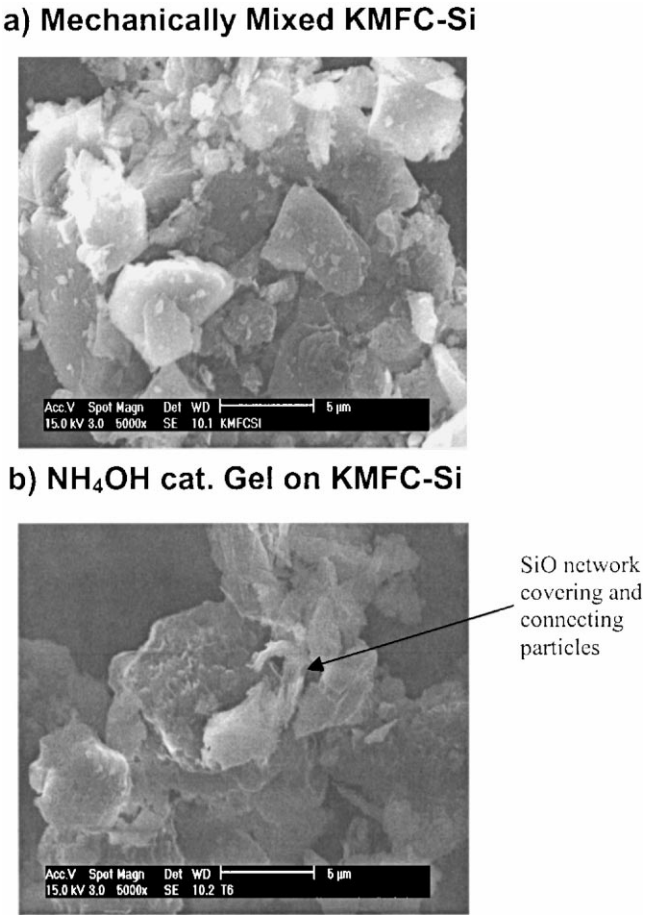

Fig. 5. Electron micrographs at 5000× magnification of: (a) mechanically mixed KMFC–Si; (b) NH_4OH-catalyzed gel on KMFC–Si.

conductivity areas over the electrode surface. This caused an overall reduction in the irreversible specific capacity, as well as better cycleability. The small fragments present in the mechanically mixed KMFC–Si mixture, which were probably fragmented graphite particles, could serve as conductivity agents in addition to the 5 wt.% of carbon black additive. On the other hand, there were no free graphite particles in the sol–gel derived composites, and the –Si–O– network restrained particle diminution. Larger agglomerates were formed which were unable to act as conductivity agents. The conductivity agents in these samples were thus limited to the 5 wt.% of carbon black added.

High magnification, 5000×, electron micrographs are shown in Fig. 5. For the mechanical mixture of KMFC–Si, the smaller particles appear to be attached loosely on the larger particle in the background. For NH_4OH-catalyzed gel on KMFC–Si, a third component (the Si–O gel material) connecting the particles together can also be seen.

4. Conclusions

In this study, graphite–silicon mixtures encapsulated in a Si–O network derived from sol–gel transformation were tested as possible negative electrode materials for lithium-ion batteries. The Si–O network increases the resistance of the KMFC–Si composite which leads to a lowered Li:Si ratio ($Li_{1.15}Si$) compared with a KMFC–Si mixture without the gel material ($Li_{2.82}Si$). Samples from NH_4OH-catalyzed sol–gel transformation are found to cycle better than samples from HCl-catalyzed reactions. This is attributed to the higher mechanical integrity of the cross-linked polymer produced by the base-catalyzed reactions as opposed to the linear polymer obtained by the acid-catalyzed sol–gel transformation.

For NH_4OH-catalyzed, gel-encapsulated graphite–silicon composites, a reversible capacity of $\sim$500 mA h g^{-1} was obtained in the first few cycles. Upon cycling to 30 cycles or more, however, this capacity decreased to below 200 mA h g^{-1}.

Though this work failed to indicate any practical advantage of the composites prepared this way over conventional carbon-based materials, the approach of containing the volumetric changes of silicon should not be dismissed completely. This is because the structure of the network depends on factors such as water to solvent ratio, temperature, catalyst utilized, etc. [15] and the gel material might not have been optimized in this study.

References

[1] B. Simon, S. Flandrois, K. Guerin, A. Fevrier-Bouvier, I. Teulat, P. Biensan, J. Power Sources 81/82 (1999) 312.
[2] M. Winter, J.O. Besenhard, M.E. Spahr, P. Noval, Adv. Mater. 10 (1998) 10.
[3] S. Bourderau, T. Brousse, D.M. Schleich, J. Power Sources 81/82 (1999) 233.
[4] C.S. Wang, G.T. Wu, X.B. Zhang, Z.F. Qi, W.Z. Li, J. Electrochem. Soc. 145 (1998) 2751.
[5] A.M. Wilson, J.R. Dahn, J. Electrochem. Soc. 142 (1995) 326.
[6] W. Xing, A.M. Wilson, G. Zank, J.R. Dahn, Solid State Ionics 93 (1997) 239.
[7] A.M. Wilson, G. Zang, K. Eguchi, W. Xing, J.R. Dahn, J. Power Sources 68 (1997) 195.
[8] A.M. Wilson, W. Xing, G. Zank, B. Yates, J.R. Dahn, Solid State Ionics 100 (1997) 259.
[9] D. Larcher, C. Mudalige, A.E. George, V. Porter, M. Gharghouri, J.R. Dahn, Solid State Ionics 122 (1999) 71.
[10] H. Huang, E.M. Kelder, L. Chen, J. Schoonman, J. Power Sources 81/82 (1999) 362.
[11] G.X. Wang, L. Sun, D.H. Bradhurst, S. Zhong, S.X. Dou, H.K. Liu, J. Power Sources 88 (2000) 278.
[12] G. Oskam, P.C. Searson, T.R. Jow, Electrochem. Solid-State Lett. 2 (12) (1999) 610.
[13] J. Niu, J.Y. Lee, in: Proceedings of the 10th International Meeting on Lithium Batteries, Como, Italy, 28 May–2 June 2000.
[14] W.J. Weydanz, M. Wohlfahrt-Mehrens, R.A. Huggins, J. Power Sources 81/82 (1999) 237.
[15] A.C. Pierre, Introduction to Sol–Gel Processing, Kluwer Academic Publishers, Dordrecht, 1998.
[16] International Centre for Diffraction Data, Pennsylvania, USA, Powder Diffraction File Release, 1998 (Data Sets 1–48 plus 70–85).
[17] T. Takamura, M. Saito, A. Shimokawa, C. Nakahara, K. Sekine, S. Maeno, N. Kibayashi, J. Power Sources 90 (2000) 45.